2025 IEEE International Conference on Energy Technologies for Future Grids
Wollongong, Australia, December 7-11, 2025

Semi-Empirical Modeling of Open-Cathode Proton Exchange Membrane Fuel Cells using a new Human-Behavior Inspired Optimisation Algorithm

Raveen De Silva*, Kosala Gunawardane*, Li Li*, Hassan Haes Alhelou*, Marie-Cécile Pera†
*School of Electrical and Data Engineering, University of Technology Sydney, Ultimo, NSW 2007, Australia
†Université Marie et Louis Pasteur, UTBM, CNRS, Institut FEMTO-ST, F-90000, Belfort, France
Email: Lindamulageraveen.s.desilva@student.uts.edu.au, Kosala.Gunawardane@uts.edu.au, Li.Li@uts.edu.au,
Hassan.HaesAlhelou@uts.edu.au, marie-cecile.pera@univ-fcomte.fr

***Abstract*—Open-Cathode Proton Exchange Membrane Fuel Cells (OCPEMFCs) provide a compact, less complex power source for portable and aerial applications. Their direct exposure to ambient air results in strong environmental dependencies and complex thermal water interactions. This study develops a semi-empirical modeling framework based on the Amphlett model, using the recently proposed human behavior inspired Tribal Intelligent Evolution Optimisation Algorithm (TIEOA), performing against best performing benchmark algorithms from literature. Experimental polarization data were collected from three different commercially available OCPEMFC stacks (Horizon H-100, Horizon H-500Xp, and Horizon H-1000). The proposed method achieved low sum of squared error (SSE) values and closely matched measured curves, outperforming several benchmark optimisers in accuracy. Results demonstrated the generalizability of the algorithm across the OCPEMFC stacks, providing a solid basis for accurate OCPEMFC modeling. This work addresses gaps in the literature on the above understudied OCPEMFC models and also provides a reliable foundation for future work in dynamic modeling and adaptive online parameter identification of OCPEMFC systems.**

***Index Terms*—Proton Exchange Membrane Fuel Cells (PEMFCs), Open-Cathode PEMFCs (OCPEMFCs), Semi-Empirical Modeling, Tribal Intelligent Evolution Optimisation**

I. Introduction

Proton Exchange Membrane Fuel Cells (PEMFCs) are electrochemical energy devices that convert hydrogen and oxygen into electricity, with water and heat as byproducts. Their high efficiency, compact form factor, and clean operation make them an attractive solution [1].

Open Cathode PEMFC (OCPEMFC) stacks are a unique configuration of PEMFCs for low power systems [2]. In these systems, ambient air is directly used to supply oxygen and remove excess heat. This design eliminates auxiliary components such as air compressors, humidifiers, and liquid cooling units, thereby reducing system weight, cost, and complexity. As shown in Fig. 1, air is drawn across the cathode using small axial fans, while hydrogen is supplied to the anode from a compressed gas source.

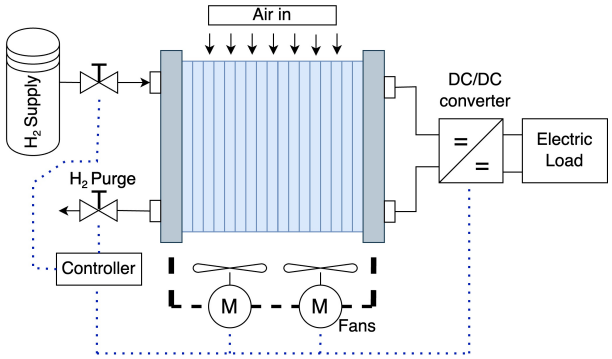

Fig. 1: Architecture of an Open-Cathode PEMFC stack.

The open cathode design is particularly attractive for applications like unmanned aerial vehicles (UAVs), robotics, and mobility, where space and weight are critical constraints [2]. OCPEMFCs operate in one of two modes: forced convection or free-breathing. Forced convection, uses fans or blowers to actively deliver air, offering better control of airflow and temperature [3], [4]. However they lack the stability of closed cathode systems, especially under variable environmental conditions. Free breathing systems, rely solely on natural convection, which are highly susceptible to performance degradation due to poor heat dissipation and limited oxygen availability. Compared to closed cathode systems, which include air preconditioning and active cooling subsystems, OCPEMFC designs face increased risks of membrane dehydration, water flooding, and uneven temperature distribution [2].

Therefore the OCPEMFC operational characteristics, and the strong dependence of OCPEMFC performance on ambient conditions, highlight the need for accurate models that can capture the system dynamics. Selecting an appropriate modeling approach is critical for performance prediction, control, and optimisation across diverse operating scenarios.

There are different PEMFC modeling approaches ranging from complex multi-dimensional computational fluid dynamics (CFD) models to simplified static and dynamic models [5], [6]. Physics-based CFD models offer high spatial resolutions

of internal processes like liquid water distribution and local species concentrations [6]. They often demand high computational resources and material properties that are difficult to obtain directly. In comparison, semi-empirical models such as the *Amphlett model* [7] offer a balanced approach, combining fundamental physics with empirical constants derived from experimental data. The hybrid nature allows for satisfactory model accuracy with reduced computational complexity, making them practical for real-time applications such as control, energy management, and fault detection. *Amphlett model* model depends on accurate parameter estimation from experimental data. This estimation requires solving a nonlinear, multi-parameter optimisation problem, where the choice of optimisation algorithm directly determines the accuracy, convergence, and reliability of the identified parameters.

Researchers have used a diverse array of metaheuristic algorithms for parameter estimation, which are analyzed based on model accuracy. Algorithms such as genetic algorithm (GA) [8], [9], supply demand optimisation (SDO) [9], harris hawks optimisation (HHO) [9], [10], whale optimisation algorithm (WOA) [11]–[13], walrus optimisation algorithm (WaOA) [13], shuffled frog leaping algorithm (SFLA) [14], grey wolf optimisation (GWO) [11], [15], parrot optimiser (PO) [12], artificial hummingbird algorithm (AHO) [15], lung performance optimiser (LPO) [13], sparrow search algorithm (SOA) [13], [15], firefly optimisation algorithm (FOA) [14], pelican optimisation algorithm (POA) [16], artificial bee colony differential evolution (ABCDE) [16] were rigorously tested across various open and close cathode type PEMFC models, such as Ballard Mark V, BCS 500 W, Stack 250 W, NedStack PS6, Horizon H-12, Temasek, Horizon-500W, and BCS-500W.

This study proposes and validates the performance of recently published Tribal Intelligent Evolution Optimisation Algorithm (TIEOA) which is a human-behavior inspired metaheuristic algorithm, for parameter estimation in the *Amphlett model*. The algorithm has been validated on 3 seperate commercially avalable OCPEMFC stacks (Horizon H-100, H-500Xp, H-1000) which are understudied and parameters not available in literature. The data collection was carried out at the University of Technology Sydney fuel cell laboratory.

This paper is organized as follows. Section II describes the semi-empirical *Amphlett model* for OCPEMFC performance simulation. Section III defines the objective function for parameter estimation. Section IV details the optimisation algorithms and their implementation. Section V outlines the experimental setup. Section VI presents the results and discussion. Section VII concludes with key findings and future research directions.

II. Formulation of the Mathematical Model

This study uses the *Amphlett model* developed by Amphlett *et al.* for the Ballard Mark IV stack in 1995 [7] which is recognized as a benchmark semi-empirical model for predicting the performance of PEMFCs. This grey-box model combines mechanistic thermodynamics with regression based polarization losses, enabling accurate fitting of steady state I–V curves (as in Fig. 2) using a compact set of empirical parameters [13]. The *Amphlett model* was chosen for its proven accuracy in predicting PEMFC performance, particularly suitable for the open-cathode designs [11], [14]. The total voltage of a stack with N series-connected cells is:

$$V_{\text{stack}} = N V_{\text{cell}}, \tag{1}$$

where each cell's voltage comprises the theoretical reversible potential minus three voltage losses as in Fig. 2:

$$V_{\text{cell}} = E_{\text{Nernst}} - V_{\text{act}} - V_{\text{ohm}} - V_{\text{conc}} \tag{2}$$

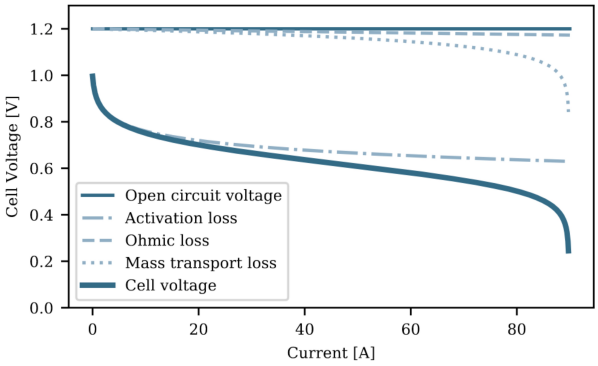

Fig. 2: I-V characteristic of a PEMFC extracted from [1]

The Nernst potential represents the theoretical reversible voltage of a PEMFC, derived from thermodynamic principles and adjusted for temperature and reactant partial pressures.

$$E_{\text{Nernst}} = 1.229 - 0.85 \times 10^{-3}(T - 298.15) + 4.3085 \times 10^{-5} T \left[\ln(P_{\text{H}_2}) + \frac{1}{2} \ln(P_{\text{O}_2}) \right], \tag{3}$$

T is temperature in Kelvin, and P_{H_2}, P_{O_2} are the effective partial pressures (atm) of H_2 and O_2, accounting for humidification and diffusion effects which are defined by equations (4) and (5) accounting for gas-phase humidification, electrochemical consumption, and mass transport losses.

$$P_{\text{H}_2} = 0.5\, \text{RH}_a P^{\text{sat}}_{H_2O} \left[\frac{P_a \exp\left(-1.635 \frac{I}{AT^{1.334}}\right)}{\text{RH}_c P^{\text{sat}}_{H_2O}} - 1 \right], \tag{4}$$

$$P_{\text{O}_2} = \text{RH}_c P^{\text{sat}}_{H_2O} \left[\frac{P_c \exp\left(-4.192 \frac{I/A}{T^{1.334}}\right)}{\text{RH}_c P^{\text{sat}}_{H_2O}} - 1 \right]. \tag{5}$$

The equations also account for relative humidity of anode and cathode(RH_a, RH_c) where temperature dependent water vapor saturation pressure ($P^{\text{sat}}_{H_2O}$) is determined by:

$$\log_{10} P^{\text{sat}}_{\text{H}_2\text{O}} = 2.95 \times 10^{-2}\, \Delta T - 9.18 \times 10^{-6}\, \Delta T^2 + 1.44 \times 10^{-7}\, \Delta T^3 - 2.18, \tag{6}$$

where the temperature offset ΔT is:

$$\Delta T = T - 273.15 \tag{7}$$

Building upon the reversible voltage in 3, below section accounts for reaction kinetics. The activation overpotential (V_{act}) represents the voltage loss due to the energy required to overcome reaction barriers in a PEMFC electrode. It is modeled empirically using four fitting coefficients ξ_1–ξ_4 as:

$$V_{\text{act}} = -\big[\xi_1 + \xi_2\, T + \xi_3\, T\, \ln(C_{O_2}) + \xi_4\, \ln(I)\big], \quad (8)$$

where the terms account for baseline loss (ξ_1), temperature effects ($\xi_2 T$), oxygen concentration dependence ($\xi_3 T \ln(C_{\text{O}_2})$), and current influence ($\xi_4 \ln(I)$). Dissolved oxygen concentration (C_{O_2}) as in 8 at the cathode liquid interface is defined by *Henry's Law* [13] as:

$$C_{O_2} = \frac{P_{O_2}}{5.08 \times 10^6 \exp\big(-498/T\big)} \quad (9)$$

The ohmic overpotential (V_{ohm}) accounts for the resistive losses due to proton conduction through the membrane and electronic resistance at cell interfaces:

$$V_{\text{ohm}} = I(R_m + R_c), \quad (10)$$

where the total resistance is the sum of membrane resistance (R_m) and contact resistance (R_c). R_m is derived from its specific resistivity ρ_m, membrane thickness l, and active membrane area A which are given by.

$$R_m = \frac{\rho_m\, l}{A}, \quad (11)$$

$$\rho_m = \frac{181.6\left[1 + 0.03\,\frac{I}{A} + 0.062\left(\frac{T}{303}\right)^2\left(\frac{I}{A}\right)^{2.5}\right]}{\left(\lambda - 0.634 - 3\,\frac{I}{A}\right)\exp\left(\frac{4.18(T-303)}{T}\right)} \quad (12)$$

This formulation reflects how membrane resistivity increases with dehydration and current loading where the water content is represented by the parameter λ. The concentration overpotential (V_{conc}) represents the voltage loss due to mass transport limitations in a PEMFC, which is modeled as:

$$V_{\text{conc}} = -\beta \ln\left(1 - \frac{J}{J_{\max}}\right), \quad (13)$$

where $J = I/A$ is the operating current density ($\text{A}\,\text{cm}^{-2}$), and $J_{\max}$ is the limiting current density (also in $\text{A}\,\text{cm}^{-2}$). The coefficient β quantifies the severity of the loss.

III. Formulation of the Objective Function

To ensure that the PEMFC mathematical model above reproduces experimental behavior of the PEMFC models under test, mathematical optimisation was done to obtain optimal values for a set of seven empirical parameters: ξ_1, ξ_2, ξ_3, ξ_4, λ, R_{con}, and β. The parameter estimation process is a nonlinear optimisation problem that minimizes the difference between experimental and modeled voltage outputs across a range of current densities. The objective function used is the sum of squared errors (SSE) between the experimentally measured voltage V_{exp} and the model-predicted voltage V_{model}, expressed as:

$$\min_{\boldsymbol{\vartheta}}\ F_{\text{obj}} = \sum_{k=1}^{N} \left[V_{\text{exp},k} - V_{\text{model},k}(\boldsymbol{\vartheta})\right]^2 \quad (14)$$

where N is the number of experimental data points, and $\boldsymbol{\vartheta} = [\xi_1, \xi_2, \xi_3, \xi_4, \lambda, R_{\text{con}}, \beta]$ is the vector of parameters to be optimised. The search space for the optimisation algorithm is constrained by lower and upper bounds for each parameter which have been used for closed cathode PEMFCs [11]–[13], [15]–[17] and open cathode PEMFCs [11], [13], [14] as summarised in Table I.

IV. Optimisation Algorithms

Solving the parameter estimation problem in Equation 14 requires a strong global optimisation method that can handle the multi parameter structure of the search space.

A. Benchmark Algorithms

GA is a popular baseline in many PEMFC parameter estimation studies, is configured with a population size N, and maximum generations equal to the iteration limit, crossover fraction used in the study is 0.8 with mutation rate $1/\dim$ [11]. SDO is the best performing method of Ref. [11], which uses an exploration probability p_{explore} decreasing linearly from 0.8 to 0.2, a step size factor α decreasing from 1 to 0. In Ref. [13], LPO, SAO, and WaOA demonstrated high performance. In this work LPO use an initial $N_e = 5$ inner cycles per iteration (increasing up to 9), an elite archive of size $\max(2, 0.05N)$, adaptive step sizes $\alpha_i \in [0.15, 0.85]$ updated via a one-fifth success rule, sinusoidal perturbations from RC parameter mapping with $f_{\text{low}} = 0.5$ and $f_{\text{high}} = 2.0$, three sequential phases (inhale/exhale, pressure flow, CO_2 separation crossover) with $2/3$ elite biased parent selection, reflection based bounds, and 0.15 probability elite exploitation using perturbation scale 0.02. SAO in the work uses $PD = 0.15$ (producer ratio), $SD = 0.25$ (aware sparrow ratio), $ST = 0.5$ (safety threshold), a linearly decreasing α ($0.5 \rightarrow 0$), and scaled Gaussian steps. Meanwhile WaOA uses an adaptive coefficient a decreasing from 2 to 0, a spiral decay factor $b = 0.5$, leader/follower/scouter ratios of $20\%/60\%/20\%$, spiral-based leader updates, Gaussian-perturbed follower moves, and 10% danger aware scouting. AHO is proposed by Ref. [15], which uses equal probability (50%) for guided and territorial foraging, Gaussian random factors $a, b \sim \mathcal{N}(0, 1)$ for step sizes, three discrete flight modes (axial, diagonal, omnidirectional) which are chosen uniformly. Also a visit table to select least recently visited food sources, and migration of every $M = 2N$ iterations to replace the worst solution with a random one.

B. Tribal Intelligent Evolution Optimisation Algorithm (TIEOA) by Yao et al.

In human societies, like-minded people cluster into tribes that compete, negotiate, and periodically unify where leaders emerge, weaker tribes vanish or are absorbed, and policies adapt from experience in a repeating cycle. This observation motivates TIEO which was proposed in 2025 by Yao *et al.* [18], which couples classification into tribes with a self-learning governance rule to search for the best "ideas" that correspond to optimal parameters.

TABLE I: Lower and upper bounds for the empirical model parameters.

Parameter	ξ_1 (V)	ξ_2 (V K^{-1})	ξ_3 (VK^{-1})	ξ_4 (V)	R_{con} (Ω)	β (V)	λ (dimensionless)
Lower Bound	-1.19969	1×10^{-3}	3.6×10^{-5}	-2.60×10^{-4}	1×10^{-4}	0.0136	10
Upper Bound	-0.8532	5×10^{-3}	9.8×10^{-5}	-9.54×10^{-5}	8×10^{-4}	0.5	24

A diverse population will be created inside the feasible box and set the shared Q table to zeros. The crowd is then split into K tribes by K means so members are close to a centroid. The leader of tribe t is the best member,

$$x_L^{(t)} = \arg\min_{x \in C_t} f(x). \tag{15}$$

Each iteration reclusters the population and every member acts using a single Q table with three choices autonomy, diplomacy, and war. Autonomy aligns a member with its leader with rare spiral exploration. Diplomacy exchanges parts with a peer then leans to the leader. War strengthens alignment with the leader while moving away from the weakest member. Exploration and step size both decay over time so the search shifts from broad probing to careful adjustment, matching the governance block in Fig. 3. At each decision the tribe records

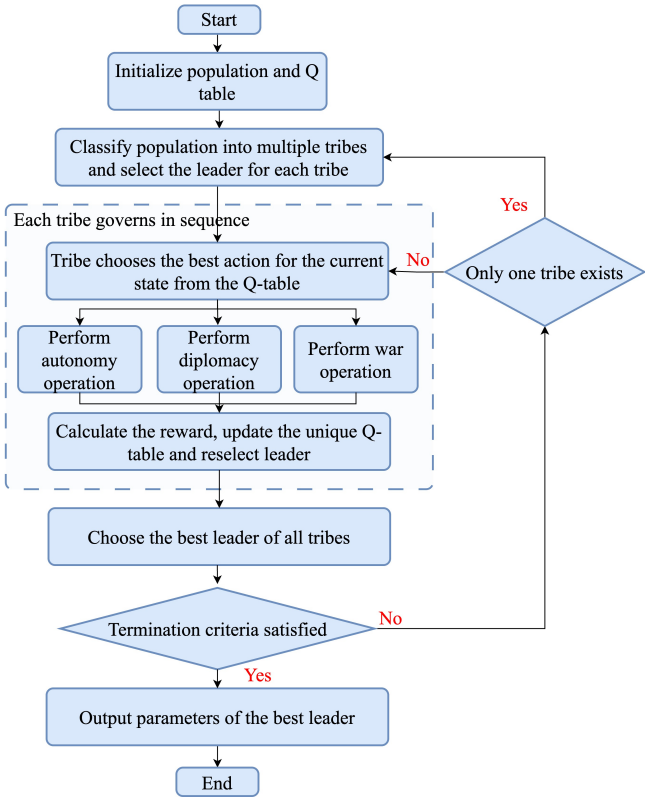

Fig. 3: TIEO algorithm adapted from Ref. [18]

a reward based on improvement and updates the Q table.

$$r_i = \max\left\{0, \frac{f_{\text{old}} - f_{\text{new}}}{|f_{\text{old}}| + 10^{-12}}\right\},$$
$$Q(s,a) \leftarrow (1-\alpha_Q)Q(s,a) + \alpha_Q\left(r_i + \gamma \max_{a'} Q(s',a')\right). \tag{16}$$

Here s encodes rank, diversity, stagnation, and phase, and s' is the next state. This is the reward and Q update step in Fig. 3. Periodically the weakest fraction in each tribe tries elite opposites and keeps an improving candidate. Stagnant members are gently reset near the global best. At merge checks the smallest tribe is scheduled for absorption and the next iteration reclusters with fewer tribes, which matches the unity decision in Fig. 3. The run ends when one tribe remains and the global best has not improved within the patience window, after which we report the best parameters, the final error, and the convergence log.

C. Ranking of the Algorithms

The performance of each optimisation algorithm was assessed using MATLAB version 2024b on an Apple M4 ARM processor. Algorithms were primarily ranked by the minimum SSE achieved, with mean, standard deviation, and worst-case SSE used as sequential tiebreakers.

V. Experimental Polarization Data Collection

The experimental data collection was performed on a test setup for the characterization of a Horizon H-500xp, H-1000 and H-100 OCPEMFCs (Fig. 4) at the University of Technology Sydney fuel cell laboratory.

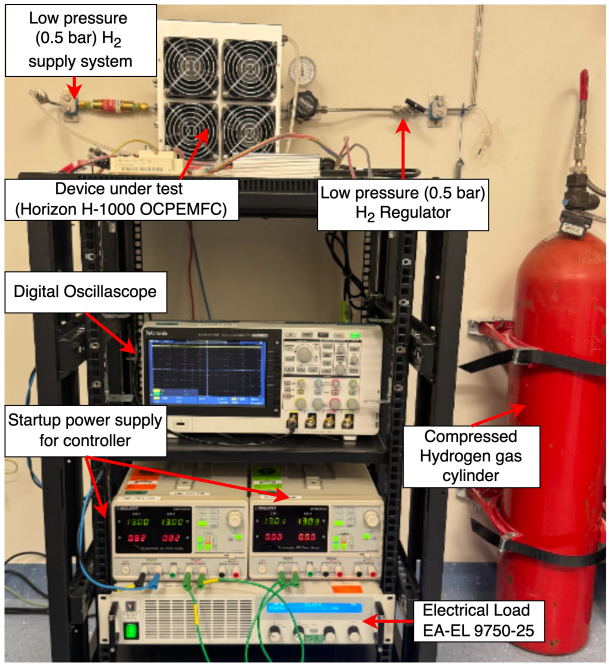

Fig. 4: Experimental setup at UTS fuel cell lab during Horizon H-1000 OCPEMFC testing.

The device under test (DUT) was fed with dry hydrogen (99.99% purity) from a compressed cylinder via a low pressure regulator set at 0.5 bar. Cathode airflow and cooling were provided by integrated axial fans with duty cycles controlled according to stack temperature through the commercial controller. A programmable electronic load (EA-EL 9750-25) applied stepwise current profiles, while voltage and current measurements were recorded. For every load change, 1 min was allowed to reach the steady state condition before recording the readings for the system to reach thermal and electrical equilibrium, which were collected over a period of 5 min at each load. It should be highlighted that in this case studies the stack temperature varies with the operating point, unlike other available case studies in the literature since the DUT is an OCPEMFC. Tests were carried out in a stable indoor laboratory environment at $18\pm1\,^{\circ}\mathrm{C}$ and 50% relative humidity, with minimal airflow disturbances.

VI. Results and Discussions

A. Case 1: Horizon H-500xp (500W PEMFC)

This case study examines the Horizon H 500xp PEMFC stack. The stack has 30 cells, a rated power of $500\,\mathrm{W}$, an active area of $76\,\mathrm{cm}^2$, a membrane thickness of $l = 25\,\mu\mathrm{m}$, and a maximum current density of $J_{\max} = 470\,\mathrm{mA\,cm}^{-2}$ [19]. Figure 5 presents the three dimensional polarization map with the experimental data, and Fig. 6 shows that absolute voltage errors which highlight the low error margin.

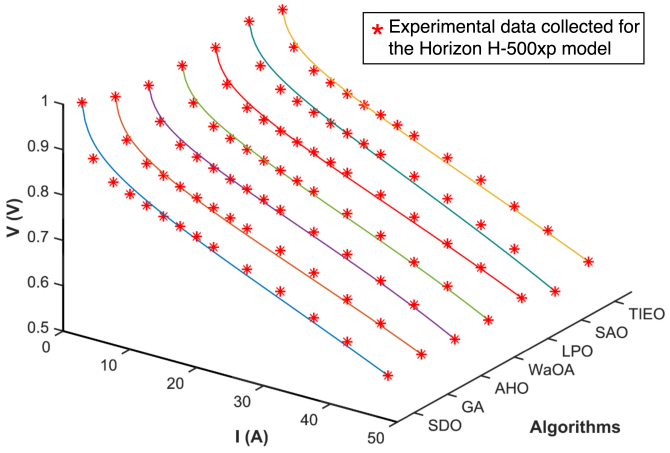

Fig. 5: Comparison of polarization curves for H-500xp.

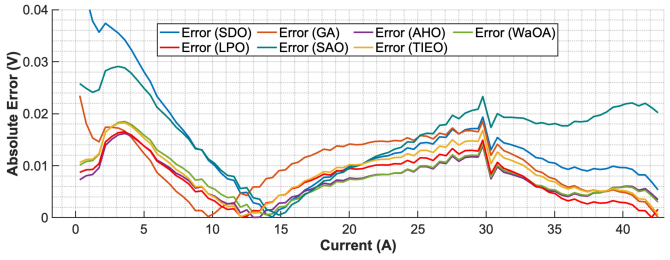

Fig. 6: Absolute error vs current for H-500xp.

The optimised parameters in Table II indicate that AHO, WaOA, and TIEO achieve nearly identical best run SSE values. Although TIEO is ranked third, the difference from WaOA and TIEO is marginal, while the other algorithms exhibit clearly larger errors.

TABLE II: Parameter values from the best run for Horizon H-500Xp OCPEMFC model.

Parameter	AHO	WaOA	TIEO
ξ_1	-1.19962	-1.19969	-1.19836
ξ_2	0.00348448	0.00390733	0.00363020
ξ_3	3.60×10^{-5}	6.66795×10^{-5}	4.68672×10^{-5}
ξ_4	-9.54×10^{-5}	-9.54×10^{-5}	-9.54×10^{-5}
R_c	0.0001000	0.0001000	0.0001000
β	0.0720770	0.0718411	0.0717708
λ	24.0000	24.0000	24.0000
Best SSE	0.0147158	0.0147176	0.0147551
Rank	1	2	3

The convergence curve in Fig.7 illustrates the reduction in the best SSE value over iterations for various optimisation algorithms applied to PEMFC parameter estimation. As shown, AHO, WaOA and TIEOA achieve faster initial convergence and lower final SSE compared to the other methods, indicating superior search efficiency and solution accuracy. The zoomed inset highlights the early iteration phase, where TIEOA demonstrates both rapid error reduction and stable convergence behavior.

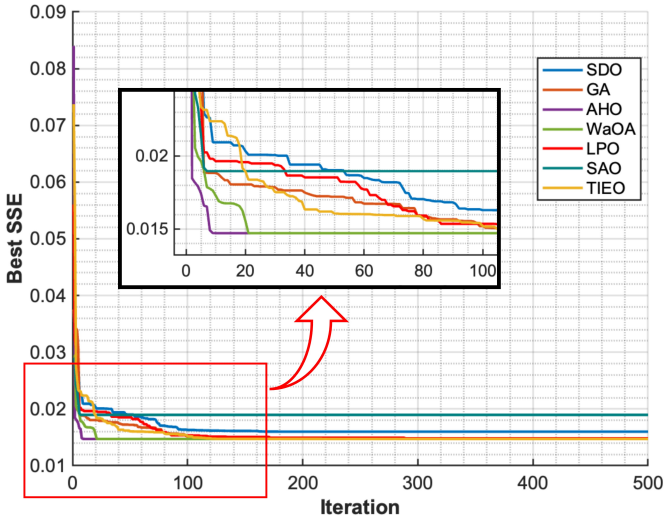

Fig. 7: Convergence curves of all optimisation algorithms showing best SSE versus iteration count for the 500 W OCPEMFC.

B. Case 2: Horizon H-1000 (1kW PEMFC)

This case study examined the Horizon H-1000 PEMFC. The stack has 48 cells, a rated power of $1000\,\mathrm{W}$, an active area of $78.4\,\mathrm{cm}^2$, a membrane thickness $l = 25\,\mu\mathrm{m}$, and a maximum current density $J_{\max} = 470\,\mathrm{mA\,cm}^{-2}$ [17]. The optimised parameters in Table III similarly indicate that AHO, TIEO, and

WaOA achieve near identical best run SSE values of 3.59451×10^{-2}.

TABLE III: Parameter values from the best run for Horizon H-1000 OCPEMFC model.

Parameter	AHO	TIEO	WaOA
ξ_1	-0.85320	-1.09312	-1.19962
ξ_2	0.00231701	0.00343956	0.00347176
ξ_3	3.60×10^{-5}	5.94253×10^{-5}	3.60×10^{-5}
ξ_4	-9.54×10^{-5}	-9.54×10^{-5}	-9.54×10^{-5}
R_c	0.0001000	0.000100006	0.0001000
β	0.124844	0.124769	0.124844
λ	24.0000	24.0000	24.0000
Best SSE	0.0359451	0.0359464	0.0359451
Mean Rank	1	2	3

C. Case 3: Horizon H-100 (100W PEMFC)

This case study examines the Horizon H-100 PEMFC stack. The stack has 20 cells, a rated power of $100\,\mathrm{W}$, an active area of $22.5\,\mathrm{cm}^2$, a membrane thickness $l = 25\,\mu\mathrm{m}$, and a maximum current density $J_{\max} = 470\,\mathrm{mA\,cm}^{-2}$ [2]. Table IV indicate that AHO, WaOA, and TIEO achieve near identical best run SSE values $\approx 3.528 \times 10^{-2}$.

TABLE IV: Parameter values from the best run for Horizon H-100 OCPEMFC model.

Parameter	AHO	WaOA	TIEO
ξ_1	-1.02694	-1.19969	-1.02689
ξ_2	0.00274733	0.00332317	0.00277433
ξ_3	3.60×10^{-5}	3.60×10^{-5}	3.79875×10^{-5}
ξ_4	-9.54×10^{-5}	-9.54×10^{-5}	-9.54001×10^{-5}
R_c	0.0001000	0.0001000	0.000100063
β	0.194326	0.194326	0.194097
λ	24.0000	24.0000	24.0000
Best SSE	0.0352818	0.0352818	0.0352832
Mean Rank	1	2	3

VII. Conclusion

This study presented a semi-empirical modeling framework for OCPEMFCs using metaheuristic optimisation techniques, with particular emphasis on the TIEOA. The methods were validated against experimental polarization data obtained from three different commercial OCPEMFC stacks under laboratory operating conditions. Across all case studies, the proposed algorithms achieved consistently low SSE values and closely matched experimental polarization curves, demonstrating their capability for accurate parameter estimation in the Amphlett model. Across all three stacks, AHO, WaOA, and TIEO achieved SSE values within 4×10^{-5} of each other (H-500Xp: 1.47158×10^{-2}–1.47551×10^{-2}; H-1000: 3.59451×10^{-2}–3.59464×10^{-2}; H-100: 3.52818×10^{-2}–3.52832×10^{-2}), confirming negligible deviation and a well-defined global minimum, hence the OCPEMFC parameter accuracy can be justified. The results highlight the robustness and generalizability of the approach across varying stack sizes and power ratings. These findings support the applicability of TIEOA-based modeling in the design, control, and diagnostics of OCPEMFC systems, and also contribute to the accurate modeling of OCPEMFC models that remain relatively understudied in the existing literature, thereby addressing a notable research gap and providing a foundation for future advancements in this domain.

References

[1] S. Heindorf Sønderskov, "Predicting Performance Degradation of Fuel Cells in Backup Power Systems."

[2] S. Strahl, N. Gasamans, J. Llorca, and A. Husar, "Experimental analysis of a degraded open-cathode PEM fuel cell stack," vol. 39, no. 10, pp. 5378–5387.

[3] D. T. Santa Rosa, D. G. Pinto, V. S. Silva, R. A. Silva, and C. M. Rangel, "High performance PEMFC stack with open-cathode at ambient pressure and temperature conditions," vol. 32, no. 17, pp. 4350–4357.

[4] J. C. Kurnia, B. A. Chaedir, A. P. Sasmito, and T. Shamim, "Progress on open cathode proton exchange membrane fuel cell: Performance, designs, challenges and future directions," vol. 283, p. 116359.

[5] F. J. Asensio, J. I. San Martín, I. Zamora, G. Saldaña, and O. Oñederra, "Analysis of electrochemical and thermal models and modeling techniques for polymer electrolyte membrane fuel cells," vol. 113, p. 109283.

[6] L. Marcelli, D. Chamoret, X. François, Y. Meyer, and D. Candusso, "Mechanical models and simulations of PEMFCs: A comprehensive review," vol. 136, pp. 1086–1111.

[7] J. C. Amphlett, R. F. Mann, B. A. Peppley, P. R. Roberge, and A. Rodrigues, "A model predicting transient responses of proton exchange membrane fuel cells," vol. 61, no. 1, pp. 183–188.

[8] N. Rajasekar, B. Jacob, K. Balasubramanian, K. Priya, K. Sangeetha, and T. Sudhakar Babu, "Comparative study of PEM fuel cell parameter extraction using Genetic Algorithm," vol. 6, no. 4, pp. 1187–1194.

[9] A. A. Al-Shamma'a, F. A. A. Ali, M. S. Alhoshan, F. A. Alturki, H. M. H. Farh, J. Alam, and K. AlSharabi, "Proton Exchange Membrane Fuel Cell Parameter Extraction Using a Supply–Demand-Based Optimization Algorithm," vol. 9, no. 8, p. 1416.

[10] M. A. Mossa, O. M. Kamel, H. M. Sultan, and A. A. Z. Diab, "Parameter estimation of PEMFC model based on Harris Hawks' optimization and atom search optimization algorithms," vol. 33, no. 11, pp. 5555–5570.

[11] A. A. Al-Shamma'a, F. A. A. Ali, M. S. Alhoshan, F. A. Alturki, H. M. H. Farh, J. Alam, and K. AlSharabi, "Proton Exchange Membrane Fuel Cell Parameter Extraction Using a Supply–Demand-Based Optimization Algorithm," vol. 9, no. 8, p. 1416.

[12] L. Chaib, F. Z. Khemili, M. Tadj, A. Choucha, B. Namomsa, S. K. Elsayed, S. S. M. Ghoneim, and A. B. Abou Sharaf, "Parrot optimizer with multiple search strategies for parameters estimation of proton exchange membrane fuel cells model," vol. 15, no. 1, p. 8802.

[13] A. A. Rathod, P. Sharma, A. Choudhary, S. Raju, and B. Subramanian, "An efficient framework for proton exchange membrane fuel cell parameter estimation using numerous MH algorithms," vol. 216, p. 115603.

[14] M. Kandidayeni, A. Macias, A. Khalatbarisoltani, L. Boulon, and S. Kelouwani, "Benchmark of proton exchange membrane fuel cell parameters extraction with metaheuristic optimization algorithms," vol. 183, no. C, pp. 912–925.

[15] P. Jangir, A. E. Ezugwu, Arpita, S. P. Agrawal, S. B. Pandya, A. Parmar, G. Gulothungan, and L. Abualigah, "Precision parameter estimation in Proton Exchange Membrane Fuel Cells using depth information enhanced Differential Evolution," vol. 14, no. 1, p. 29591.

[16] L. M. Perez, S. Jemei, L. Boulon, A. Ravey, M. Kandidayeni, and J. Solano, "Comparative study of a new semi-empirical model of the proton exchange membrane fuel cell for online prognostics applications," vol. 331, p. 119655.

[17] I. M. M. Saleh, R. Ali, and H. Zhang, "Simplified mathematical model of proton exchange membrane fuel cell based on horizon fuel cell stack," vol. 4, no. 4, pp. 668–679.

[18] Y. Yao, X. Hong, and L. Xiong, "Study on a new metaheuristic algorithm – Tribal intelligent evolution optimization and its application in optimal control of cooling plants," vol. 383, p. 125339.

[19] A. Omran, A. Lucchesi, D. Smith, A. Alaswad, A. Amiri, T. Wilberforce, J. R. Sodré, and A. G. Olabi, "Mathematical model of a proton-exchange membrane (PEM) fuel cell," vol. 11, p. 100110.